Electronic Supplementary Material (ESI) for Green Chemistry.

Supplementary Infomation

Tailored one-pot lignocellulose fractionation to maximize biorefinery toward versatile xylochemicals and nanomaterials

Yanyan Yu, Wanke Cheng, Yilin Li, Tong Wang, Qinqin Xia, Yongzhuang Liu*, Haipeng Yu*

Key Laboratory of Bio-Based Material Science and Technology of Ministry of Education, Northeast Forestry University, Harbin 150040, P. R. China.

*Corresponding Email: yuhaipeng20000@nefu.edu.cn; lyz@nefu.edu.cn

This PDF file includes:

Supplementary Materials

All the chemicals were directly used as received without any purification. Poplar sawdust was used after Soxhlet extraction (toluene/ethanol) and dried at 103 °C overnight for further use. Choline chloride (ChCl), oxalic acid dihydrate (OA) and diols including ethylene glycol (EG), 1,3-propylene glycol (PG), 1,4-butanediol (BD) and 1,5-pentanediol (PD) used for the preparation of deep eutectic solvents (DESs) were purchased from Aladdin Reagent Co., Ltd. (Shanghai, China). Ethanol and distilled water were used for components separation workup.

Supplementary Methods

1.1 Calculation of lignin yield and semi-quantitative analysis of substructures

The yield of the isolated diol-alkoxylated lignins was corrected with a correction factor as previously reported.(*1*) 2D HSQC NMR was used for semi-quantitative analysis of the obtained lignins, and relative content of the substructures was described as content per 100 aromatic units.(*1*) Detailed calculations after integral were as follows:

For the aromatic region:

$$\text{Total aromatic units} = (S_{2/6} + S'_{2/6})/2 + S_{condensed} + (G_2 + G_5 + G_6)/3 + PB/2$$

$$\text{Condensation ratio} = S_{condensed}/\text{Total aromatic content} \times 100\%$$

For the linkages in the side chain region:

$$\text{Total } \beta\text{-}O\text{-}4' \text{ linkages} = [(\beta\text{-}O\text{-}4'_{\alpha} + \alpha\text{-alkoxylated } \beta\text{-}O\text{-}4'_{\alpha})/\text{Total aromatic units} \times 100]/1.3$$

$$\beta\text{-}\beta \text{ linkages} = (\beta\text{-}\beta_{\alpha}/\text{Total aromatic units} \times 100/1.3$$

1.2 Composition analysis

The compositions of the untreated lignocellulose and DES-fractionated SRs were determined according to the National Renewable Energy Laboratory (NREL) procedure.(*2*) 0.3 g oven-dried sample was weighed in a glass bottle with a screw cap, and 3 mL 72 wt% H_2SO_4 was mixed with the sample with continuous stirring for 1 h, then the mixture was diluted to a concentration of 3 wt% H_2SO_4 and heated in an oven at 121 ℃ for 1 h. After cooling to room temperature, the liquid was injected into HPLC for analysis after filtration. The undissolved

solid was filtered and dried to determine the lignin content. The glucose and xylose from cellulose and hemicellulose were determined by HPLC (Agilent 1260, Agilent Technologies, USA) with a refractive index detector (RID). An amine column HPX-87H (Bio-Rad, USA) was used to analyze the glucose and xylose at 50 ℃ with 4 mM sulfuric acid as mobile phase, and the flow rate was 0.6 mL/min. The yield of monosaccharides was calculated by calibration of the standards. Glucose and xylose were used to calculate the yield of cellulose and hemicellulose, respectively. Acid insoluble lignin was used to calculate the lignin content in original lignocellulose or fractionated SRs. The ash content in poplar wood was determined by counting the mass of the residues remaining after the sample was heated in a muffle furnace at 550 ℃.(*3*) The average ash content was calculated from three measurements.

1.3 Preparation of milled wood lignin (MWL)

Typically, 20 g poplar sawdust was milled in a planetary ball mill for 2 h and then mixed with 96 wt% dioxane solution with a ratio of 1:20 g/mL. The mixture was stirred under ambient temperature and dark condition for 24 h. The reacted mixture was centrifuged at 5000 rpm and the residue was washed with 96 wt% dioxane solution. A combination of centrifuged liquid and washed liquid was concentrated to about 30 mL by rotary evaporation (50 ℃). The obtained mixture was added dropwise into 3 times volume of ethanol solution (96%). After filtration, the filtrate was concentrated and precipitated in the same ethanol solution twice. Finally, the ethanol solution mixture was concentrated to 30 mL and added dropwise into 10 times volume of acidic aqueous solution (pH = 2), and the mixture was filtered and dried to obtain the mill wood lignin (MWL) sample.(*4*, *5*)

1.4 Quantitative ^{31}P NMR analysis of the DES-fractionated lignin

Quantitative ^{31}P NMR was performed according to the literature.(*6*) 2-Chloro-4,4,5,5-tetramethyl-1,3,2-dioxaphospholane was used as a phosphitylating reagent. Generally, 30 mg lignin was dissolved in 0.5 mL anhydrous deuterated pyridine and deuterated chloroform (1.6:1 v/v) with continuous stirring. 0.1 mL cyclohexanol (~10.85 mg/mL) as internal standard and 0.1 mL chromium(III) acetylacetonate solution (5 mg/mL in anhydrous deuterated pyridine and deuterated chloroform 1.6:1, v/v) as relaxation reagent were added into the mixture. Finally, the mixture was reacted with 0.1 mL phosphitylating reagent for 10

min, and the obtained mixture was transferred into the NMR tube for analysis. Standard ^{31}P sequence was selected from Bruker Program Library with total scans of 1024.

1.5 Hydrogenolysis of the isolated lignin to aromatic monomers

The hydrogenolysis of lignin was performed using hydrogen transfer method as described.(*7*) Typically, 0.1 g CO-L or COPD-L was used as the raw material, representing condensed lignin and tailored less-condensed lignin. 0.1 g Ru/C (5% loading) as catalyst, 10 mL ethylene glycol as solvent and 30 mg 2-isopropylphenol as internal standard were added into a 25 mL autoclave with a glass insert. The autoclave was sealed and heated to 190 ℃ with continuous stirring for 6 h. After cooling to room temperature, the mixture was filtered and extracted with dichloromethane and water. The results were qualitatively and quantitatively analyzed by GC/MS and GC-FID, respectively. *Para*-propylguaiacol was used for calibration, and the response factor for other monomers was determined by the effective carbon number method.(*8*) The calculated response factor for *para*-propylsyringol was 1.42.

1.6 Synthesis of printing resin using the isolated lignin as polyols

COPD-L was used to investigate the possibility of directly using the isolated lignin instead of conventional aromatic polyols for printing ink resin, and the procedure for resin synthesis was referred from the literature with slight modification.(*9*) Typically, 17 mmol (5.24 g) abietic acid and 8 mmol (0.76 g) maleic anhydride were mixed in a 250 mL round flask at 180 ℃ for 2 h under nitrogen atmosphere. After reaction, total 24 mmol polyols (1g COPD-L and 2.2 g glycerol) were added into the flask and heated to 260 ℃ for 2 h, and the resin for printing ink was obtained after cooling to room temperature. A varnish for printing ink was obtained by adding Linseed oil and methyl oleate into the obtained resin (resin: Linseed oil: methyl oleate = 40:20:40 % mass percentage). The patterns were obtained by simply printing the varnish using a microelectronic printer (Scientific 3A electronic printer, Mifang Electronic Technology Co. LTD, Shanghai).

1.7 Determine the yields of enzymatic hydrolysis monosaccharides by HPLC

Enzymatic hydrolysis of the SRs was performed as follows: 0.3 g oven-dried sample was weighed in a 50 mL centrifuge tube with cap, and then 7.5 mL sodium acetate buffer (50 mmol/L, pH 5.5) followed by 2.88 mg tetracycline chloride. The tube was kept at 50 ℃ in an

incubating orbital shaker at 300 rpm for 96 h. Enzymatic hydrolysis was conducted with Cellic® CTec2 (Novozymes, Denmark, 145 FPU/mL, ~30 FPU/g glucan) and 0.2 mL hydrolysate was sampled periodically to determine the released monosaccharides amount in liquid phase after inactivation of the enzyme (110 ℃, 5 min). The glucose and xylose were determined by HPLC (Agilent 1260, Agilent Technologies, USA) with an autoinjector and RID detector. An HPX-87H (Bio-Rad, USA) with a 4 mM H_2SO_4 mobile phase at 0.6 mL/min was used.

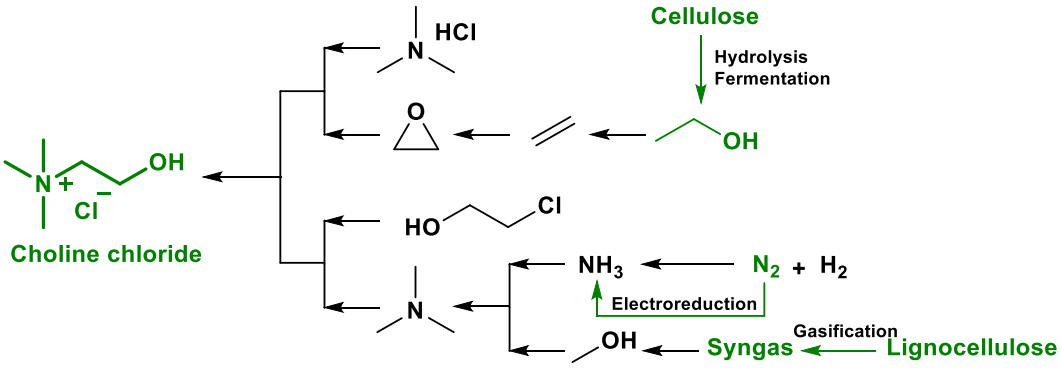

Fig. S1 Synthetic route for choline chloride and possible alternatives from lignocellulose.(*10–12*)

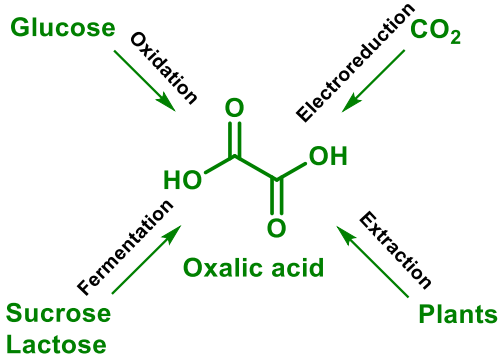

Fig. S2 Green synthetic route for bio-derived oxalic acid.(*13–16*)

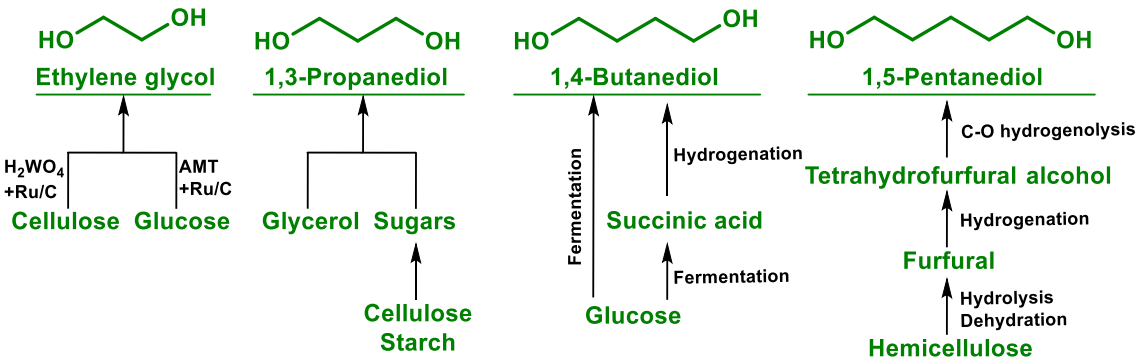

Fig. S3 Synthetic route for C2–C5 diols from carbohydrates.(*17–23*)

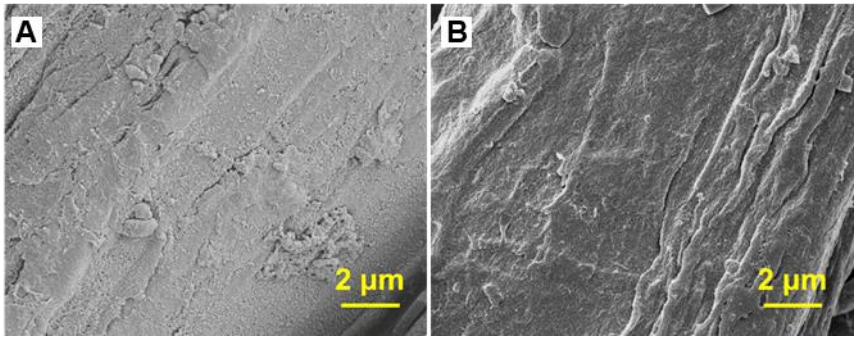

Fig. S4 SEM images of CO-SR (A) and COEG-SR (B) at low magnification. On the surface of CO-SR, a lot of particles were observed even at low magnification, while the COEG-SR showed a typically clean and fibrous surface.

Fig. S5 Digital images of the isolated CO-L and COEG-L. the dark color of CO-L revealed a severe condensation of lignin as previously described while COEG-L showed a light brown color, demonstrating that the lignin was less condensed due to the tailoring effect of EG.

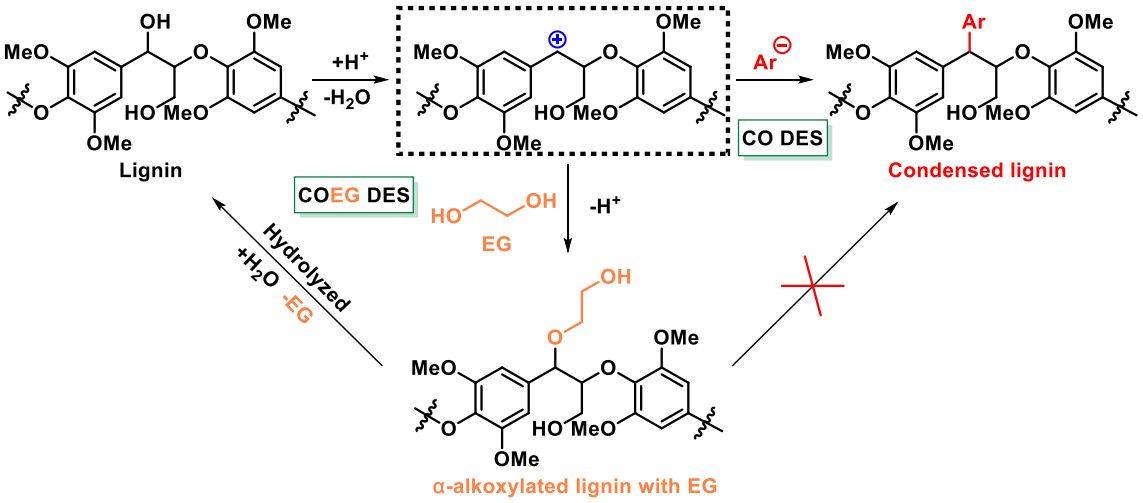

Fig. S6 Proposed reaction pathways of lignin in CO (condensed lignin) and COEG (*α*-alkoxylated lignin derivative). In CO, the acidity of the system was strong enough to cleavage all the ether bond in lignin, and the active carbocation intermediates would condense to form recalcitrant C–C bonds. In COEG, EG in the system would react with the carbocation intermediates through alkoxylation, and the condensation pathway would be effectively suppressed.

Fig. S7 Digital images of COPA-SR (left) and COPD-SR (right). The SR from COPA fractionation system showed a darker color than the COPD system, revealing that the hydroxy rich PD molecules can promote delignification, possibly due to the hydrogen bond formation between alkoxylated lignin and DES.

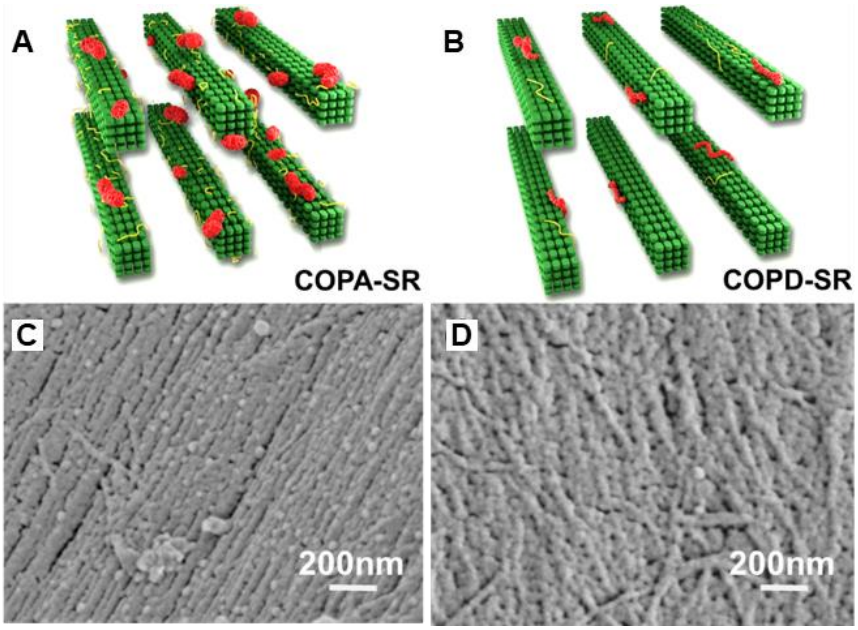

Fig. S8 Schematic diagrams and SEM images of COPA-SR (A, C) and COPD-SR (B, D) at high magnification. The lignin obtained from COPA fractionation would be alkoxylated with alkyl tails, leading to poor delignification, and the remained lignin would be dispersed in the cellulose matrix. When PD was used instead of PA with one more equivalent hydroxy, the lignin would be alkoxylated with aliphatic tails, and excellent delignification was achieved possibly due to the hydrogen bonding formation of the hydroxy tails with DES, hence enhanced lignin removal, and the SRs showed a rather clean and fibrous structure.

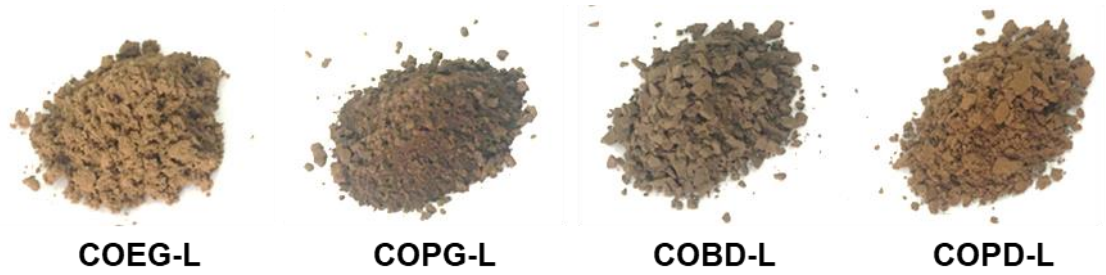

Fig. S9 Digital images of isolated COEG-L, COPG-L, COBD-L and COPD-L. All the lignin fractions from the diol-tailored DES fractionation showed lighter color than that of CO-L, revealing less condensation.

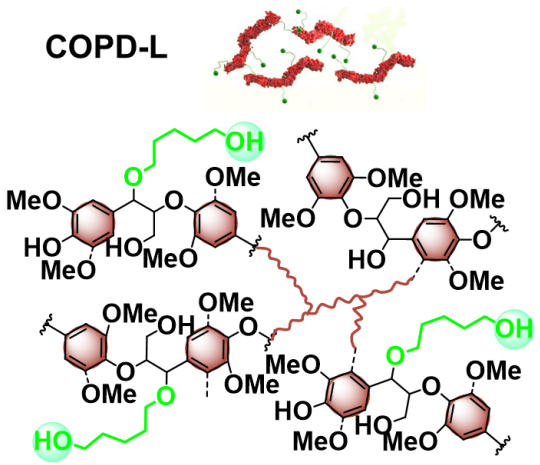

Fig. S10 Proposed structure of hydroxyl rich and aryl ether retained COPD-L. According to the NMR studies, possible lignin structure (COPD-L as example) was proposed, demonstrating an aryl ether bond retained linkages, and the obtained lignin was also functionalized with long aliphatic hydroxy tails.

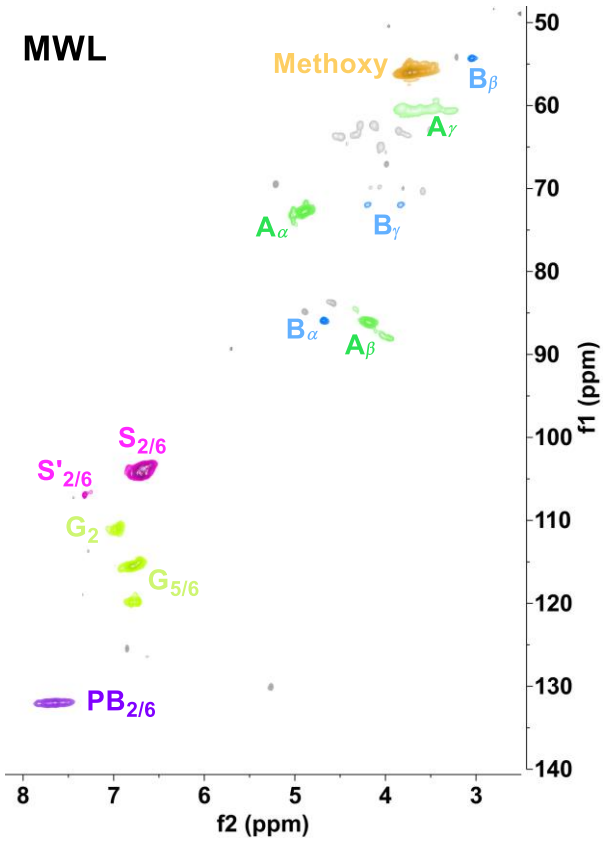

Fig. S11 The 2D HSQC NMR spectrum of MWL.

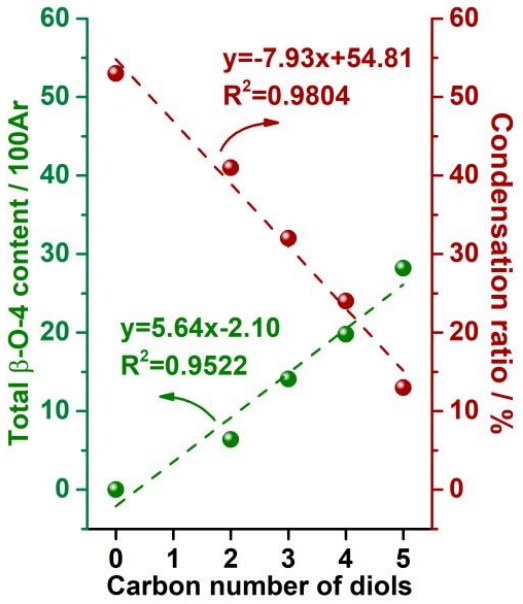

Fig. S12 Correlation between carbon number in diols and β-*O*-4' content and condensation ratio of fractionated lignin. Note: CO-L with carbon number of 0 is also included for correlation.

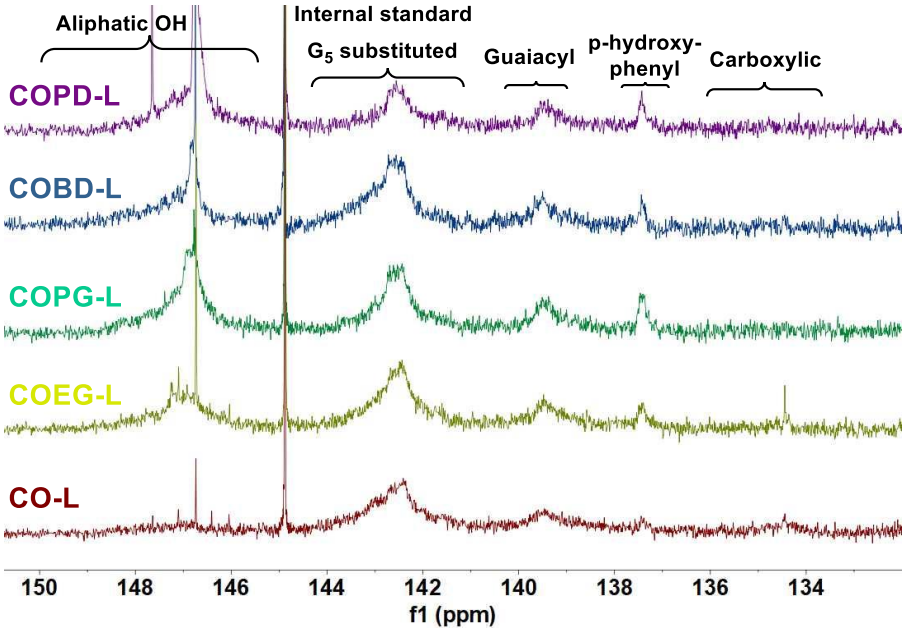

Fig. S13 ^{31}P NMR spectra of the fractionated lignin. The spectra were assigned and analyzed according to the literature.(*6*) Cyclohexanol is used as internal standard.

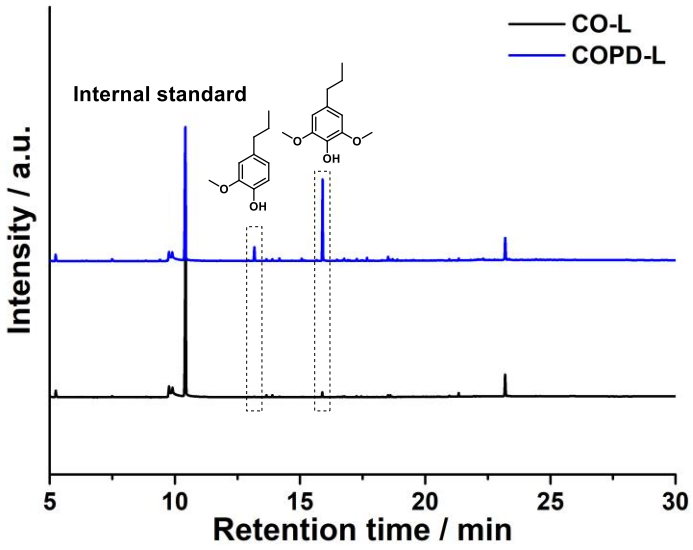

Fig. S14 GC-FID spectra of products after CO-L and COPD-L depolymerization. 2-Isopropylphenol was used as internal standard.

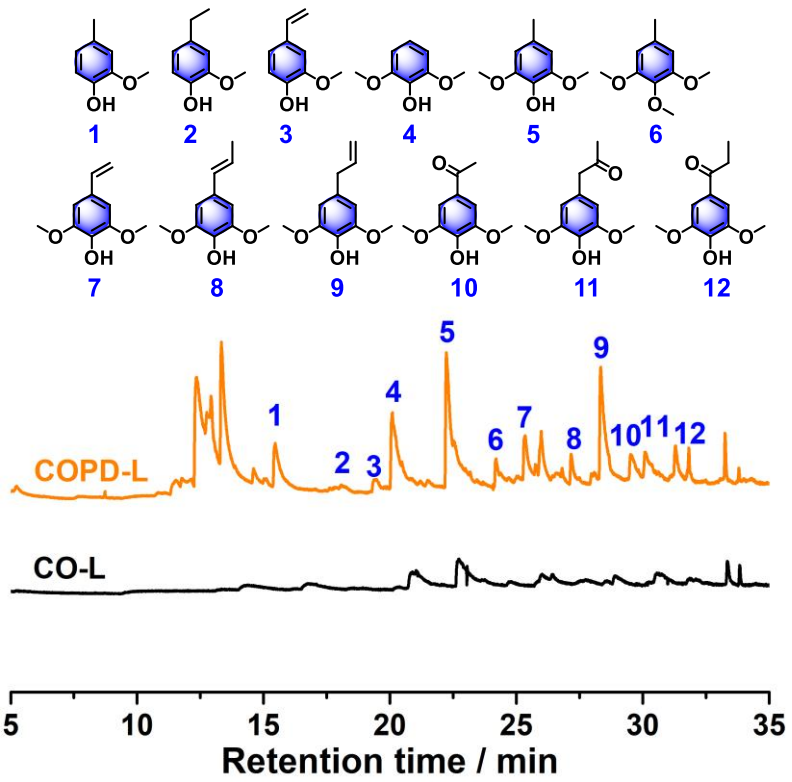

Fig. S15 Pyrolytic lignin monomer distribution from Py–GC/MS analysis.

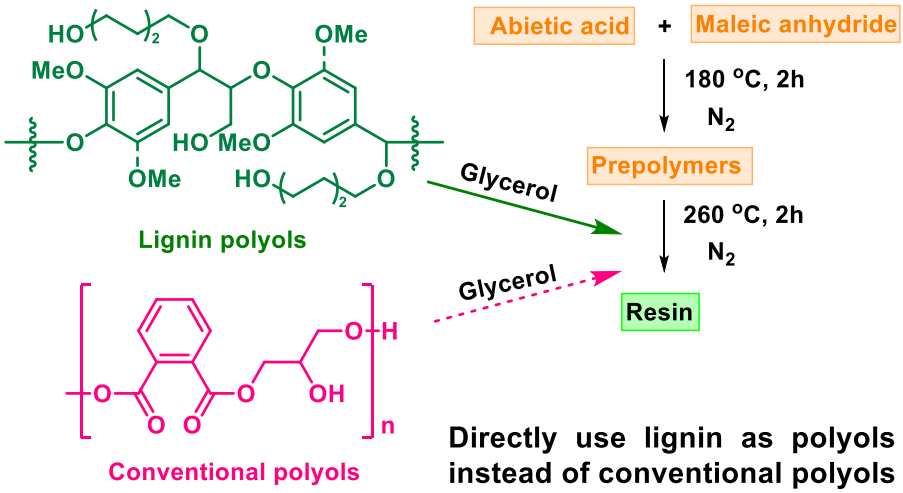

Fig. S16 Synthesis of resin for printing ink using natural polyols instead of conventional aromatic polyols.

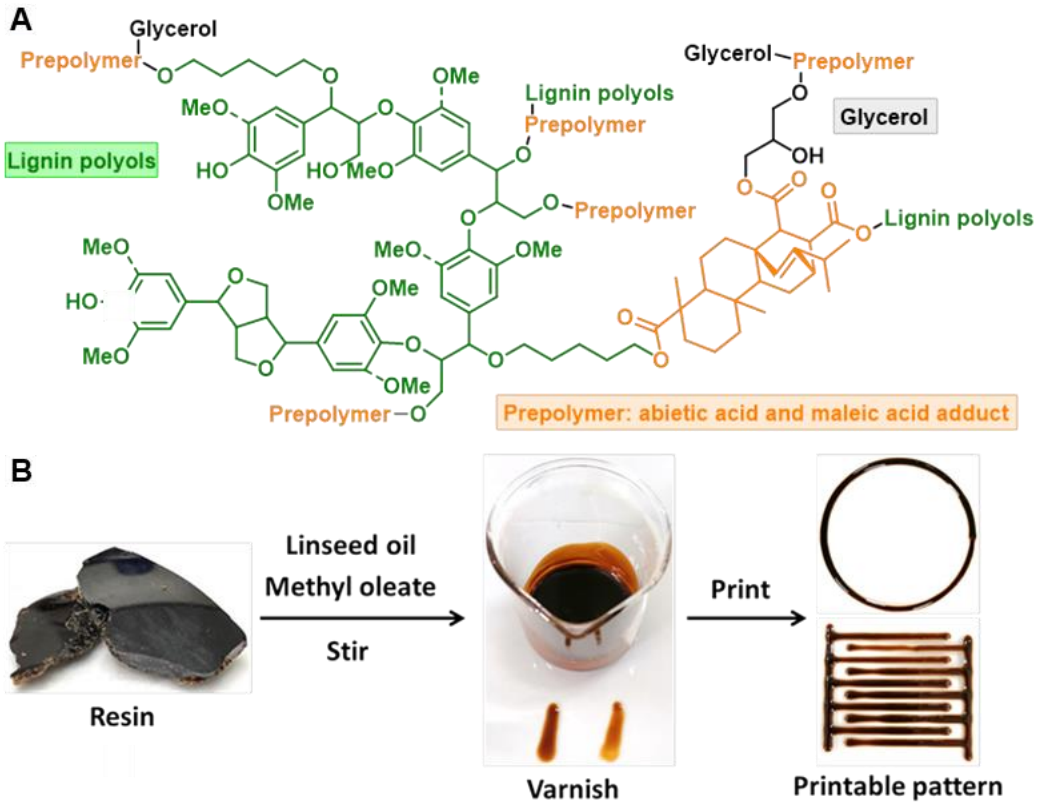

Fig. S17 (A) Proposed molecular structure of the resin for printing ink; (B) digital images of resin for printing ink, varnish, and printable pattern by microelectronic printer (Scientific 3A electronic printer, Mifang, Shanghai).

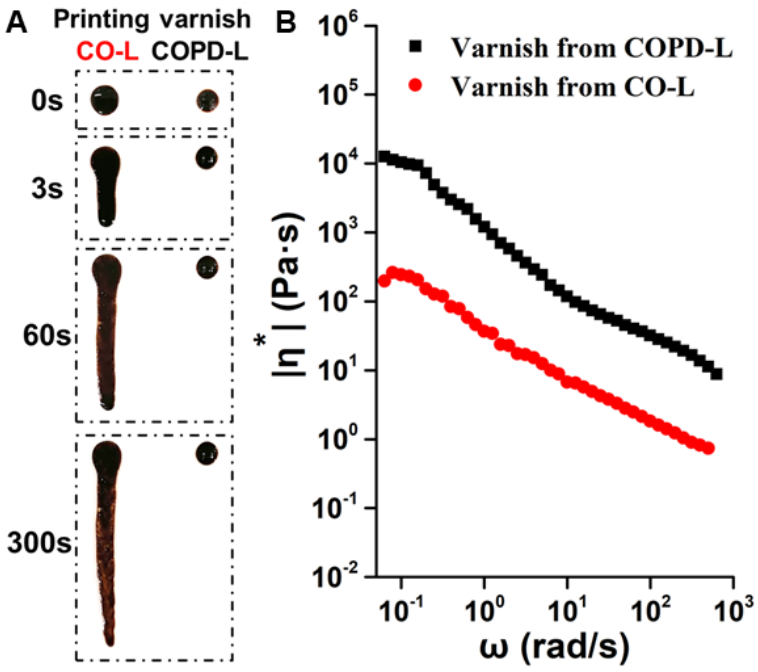

Fig. S18 Digital images of the fluidity (A) and viscosity (B) test of printing varnish from CO-L or COPD-L.

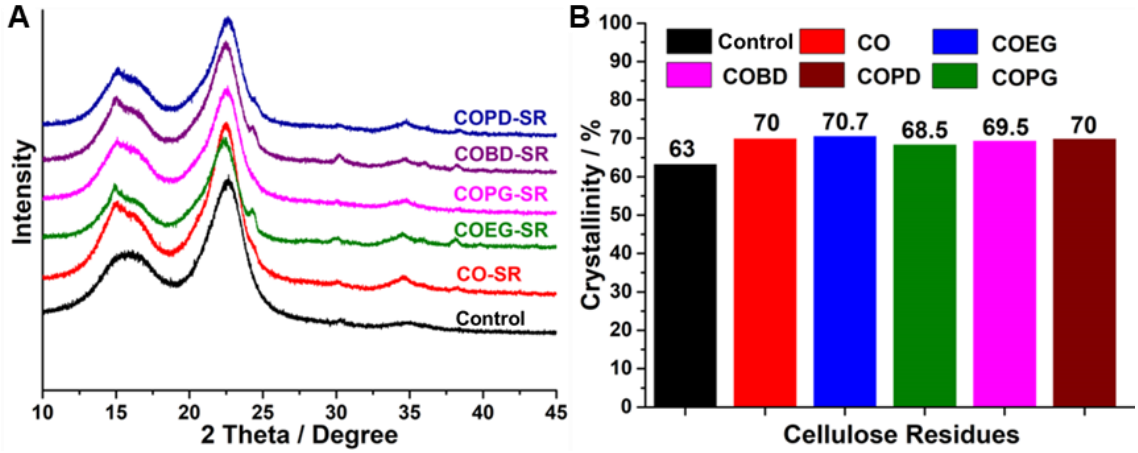

Fig. S19 XRD curves (A) and crystallinity (B) of the SRs. The crystallinity was calculated according to the Segal's method.(*24*)

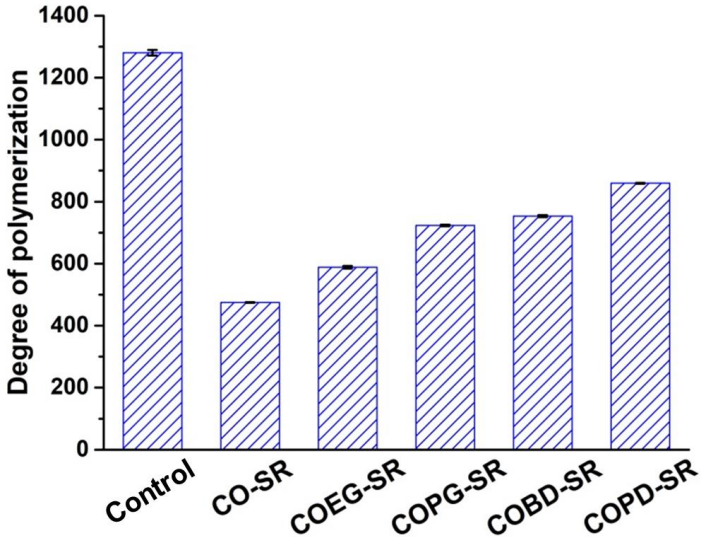

Fig. S20 Degree of polymerization (DP) of raw lignocellulose and fractionated SRs. The degree of polymerization was measured by Ubbelohde viscometer.

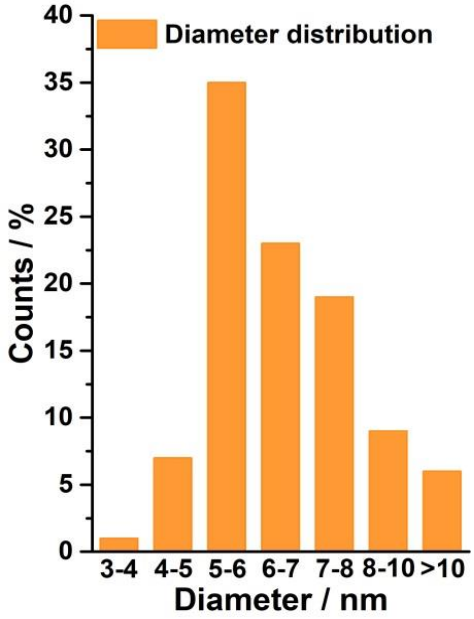

Fig. S21 Diameter distribution of cellulose nanofibers from COPD-SR, which was measured from TEM images using a TDY-V5.2 image analysis system (Tianhong Precision Instruments, Beijing, China).

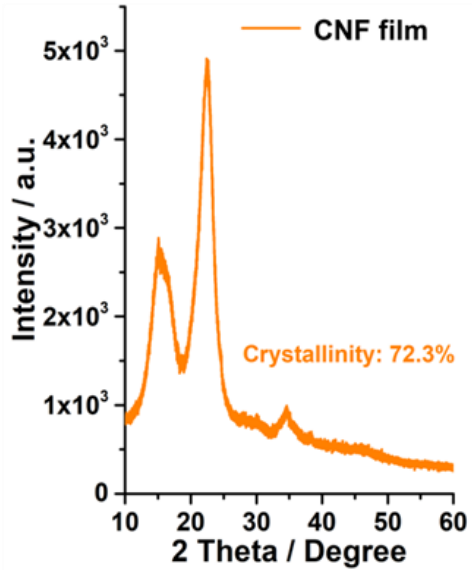

Fig. S22 XRD analysis of the obtained cellulose nanofiber film.

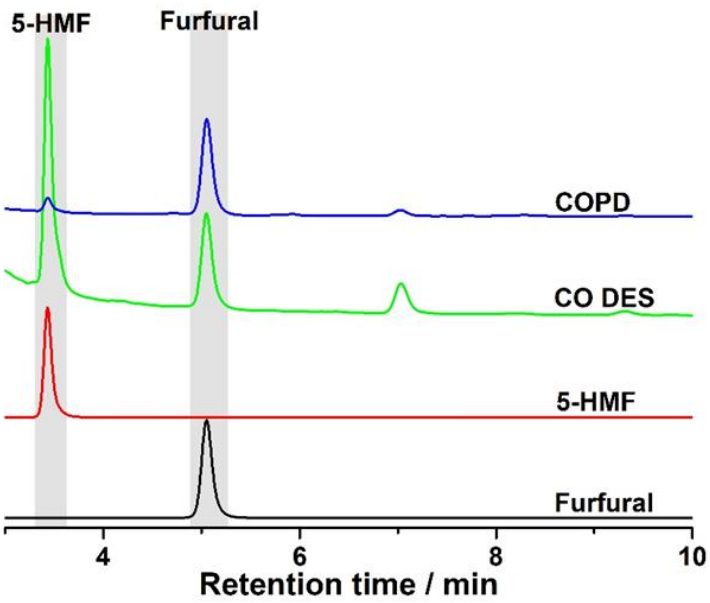

Fig. S23 HPLC analysis of furfural and 5-HMF in CO and COPD after fractionation. The mixture after fractionation was diluted with water and directly injected into HPLC after filtration for analysis. Standard 5-HMF and furfural were used to identify the products.

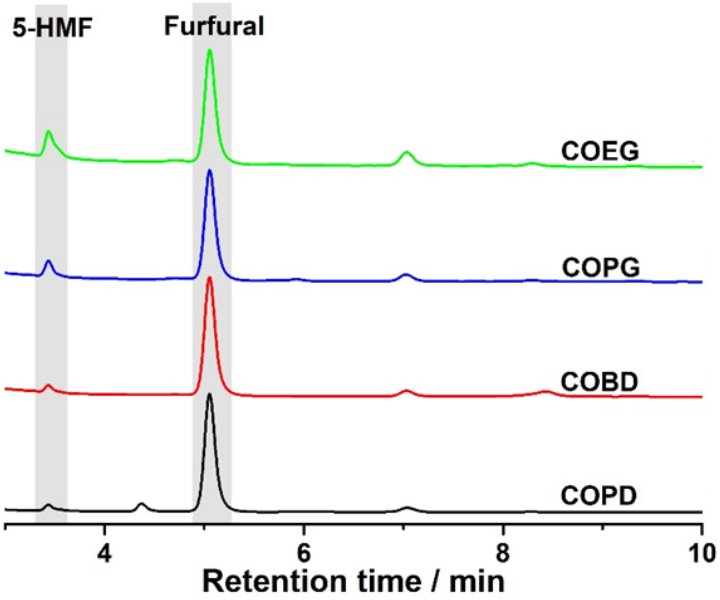

Fig. S24 HPLC analysis of furfural and 5-HMF in COEG, COPG, COBD and COPD after fractionation. The yield of furfural was determined by calibration.

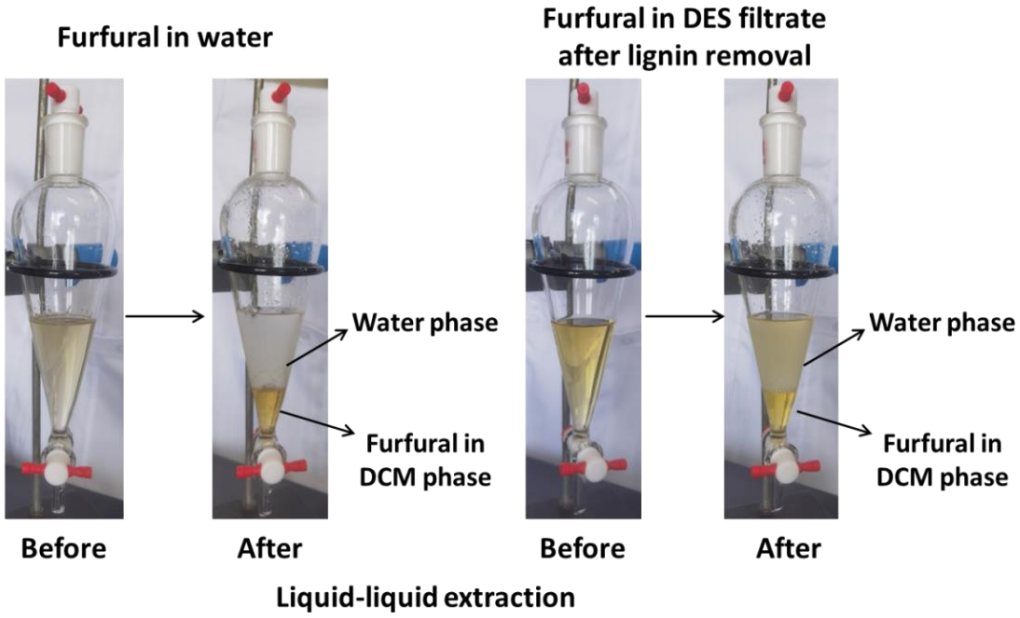

Fig. S25 Possible recovery method for furfural as well as furfural in DES filtrates by liquid–liquid extraction.

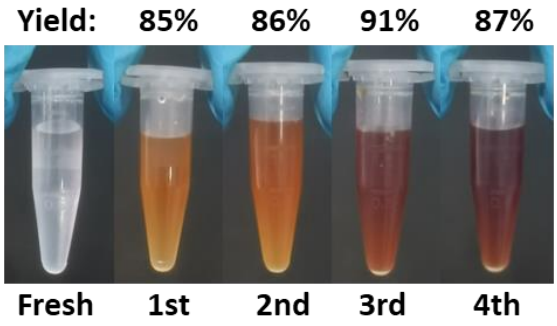

Fig. S26 Digital images and yields of fresh and recycled COPD.

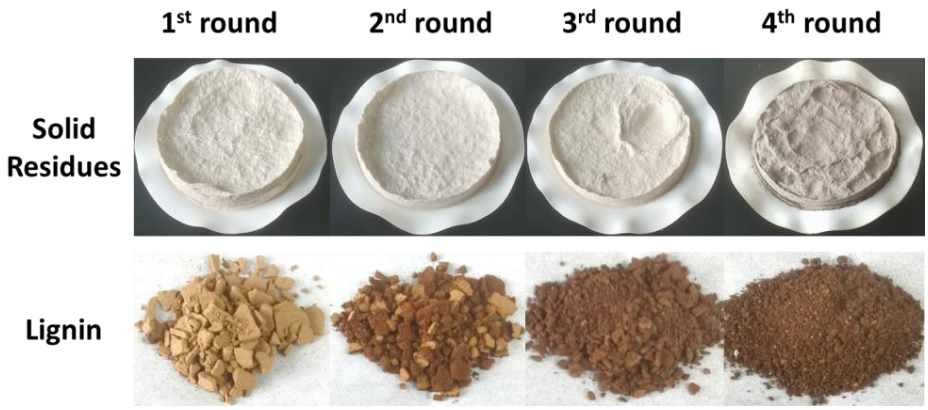

Fig. S27 Digital images of solid residues and lignins from recycled COPD fractionation.

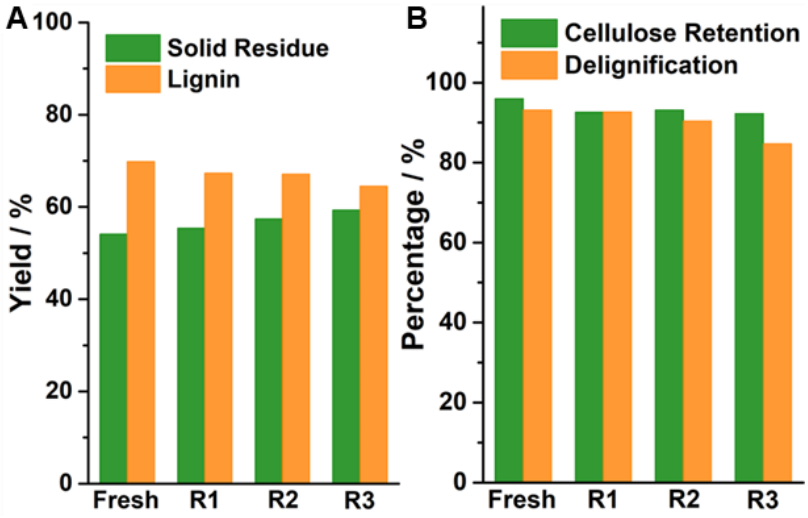

Fig. S28 Yields of solid residues and lignin (A) and percentage of cellulose retention and delignification (B) in solid residues from COPD or recycled COPD.

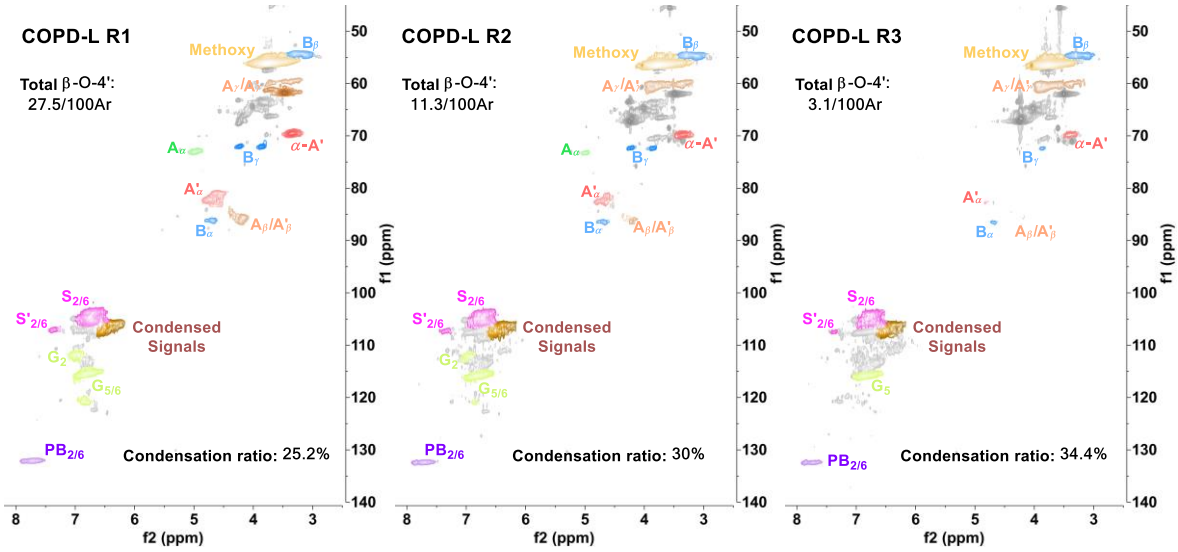

Fig. S29 2D HSQC NMR of COPD-L after different fractionations of poplar wood in recycled COPD.

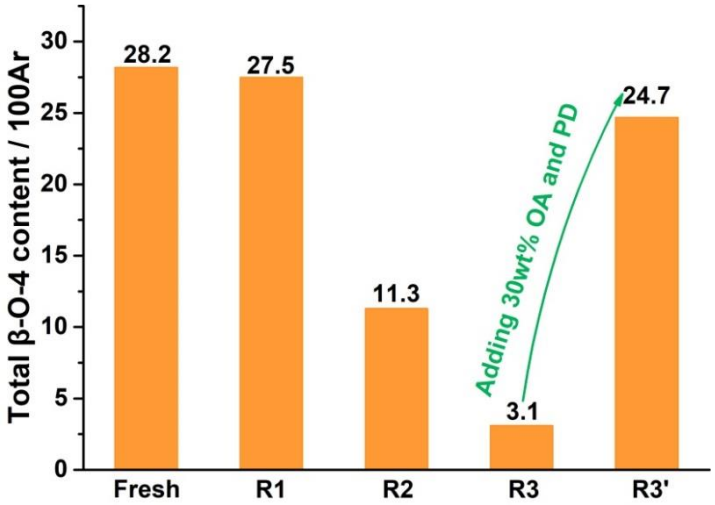

Fig. S30 Total β-*O*-4' content of lignin obtained by fractionation using fresh and recycled COPD. Analysis based on semi-quantitative 2D HSQC NMR spectra.

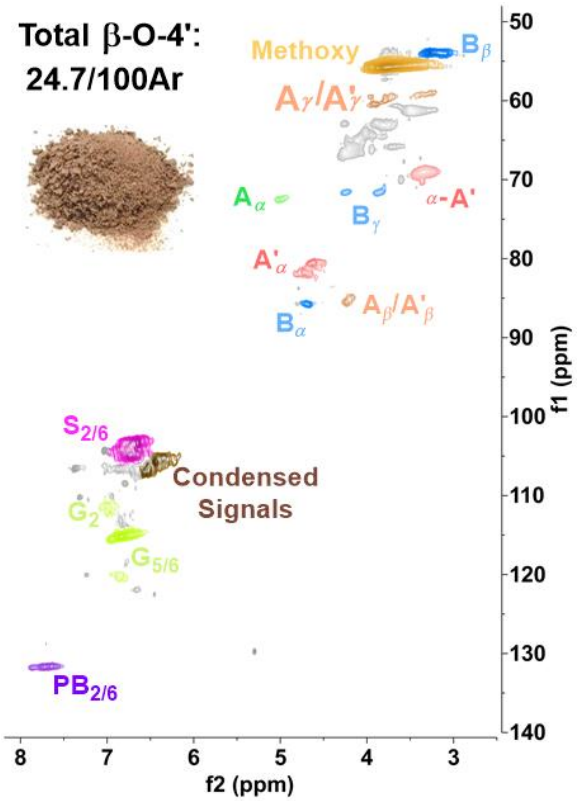

Fig. S31 2D HSQC NMR of COPD-L after fractionation of poplar wood with recycled COPD (third recycle) with the addition of 30 wt% OA and PD.

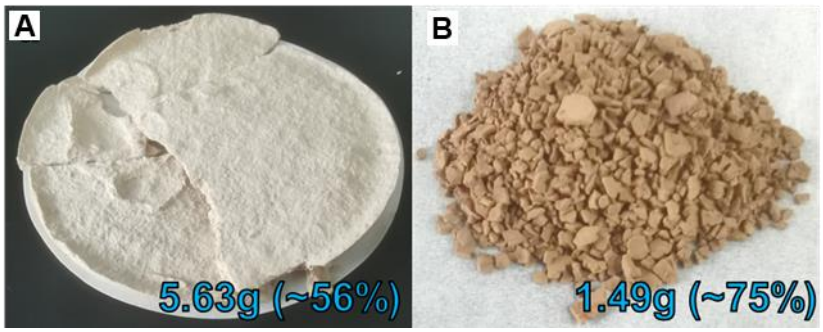

Fig. S32 Digital images of COPD-SR (A) and COPD-L (B) after fractionation of 10 g of lignocellulose in COPD.

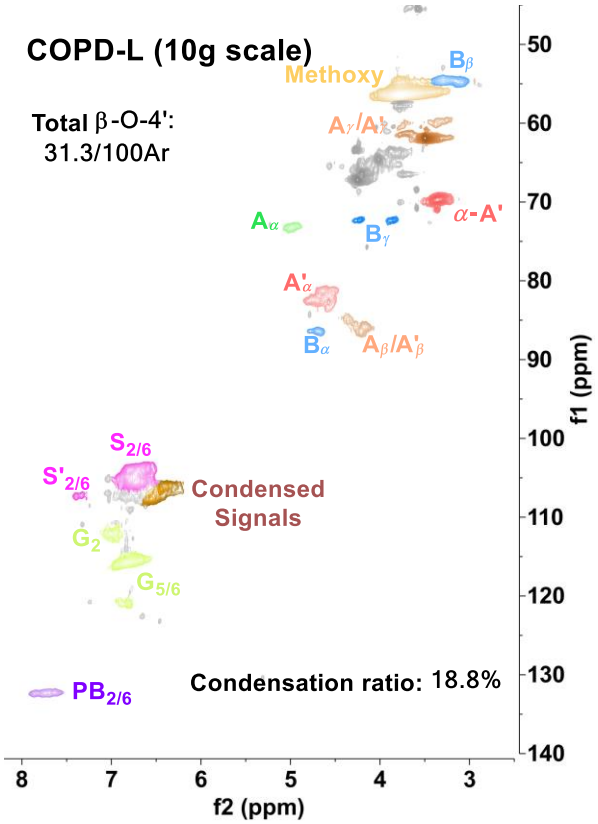

Fig. S33 2D HSQC NMR analysis of COPD-L after fractionation of 10 g of lignocellulose in COPD.

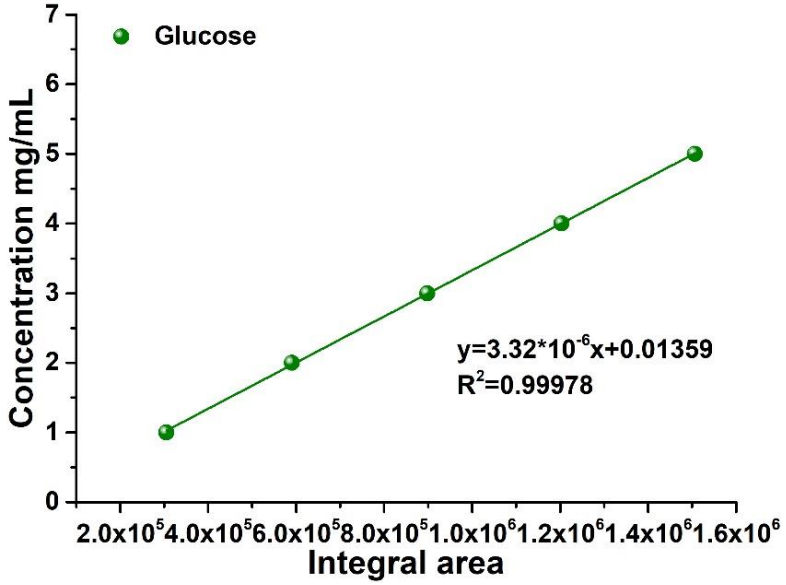

Fig. S34 Calibration curves of glucose by HPLC.

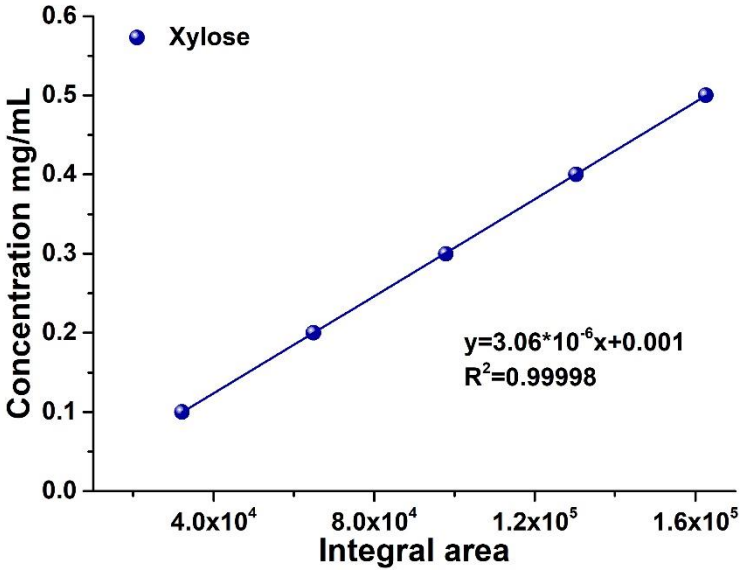

Fig. S35 Calibration curves of xylose by HPLC.

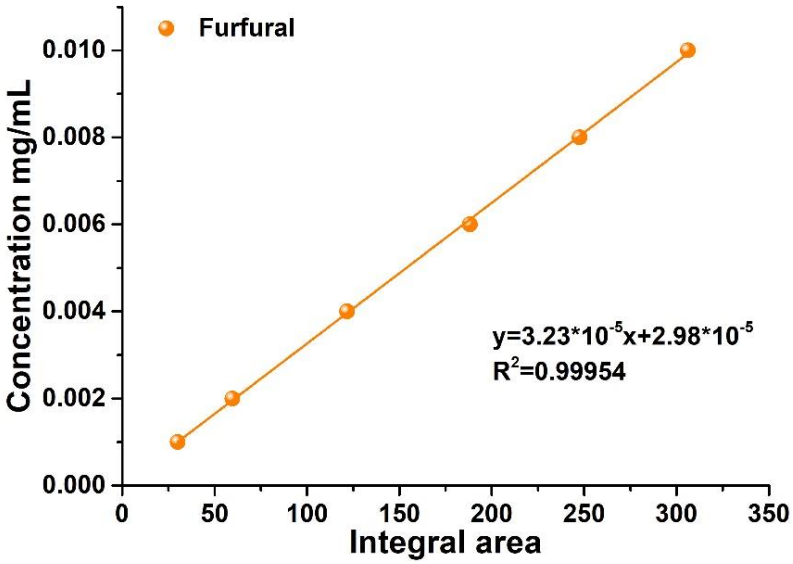

Fig. S36 Calibration curves of furfural by HPLC.

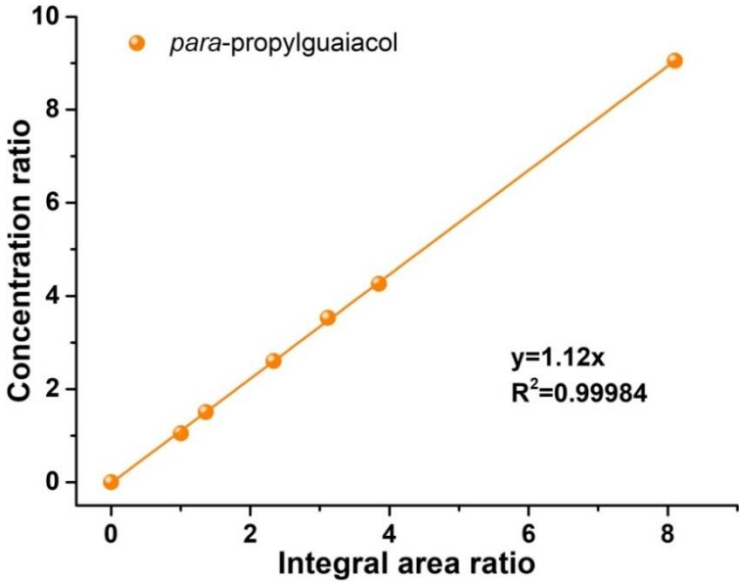

Fig. S37 Calibration curves of *para*-propylguaiacol by GC-FID using 2-isopropylphenol as internal standard.

Table S1. Comparison of DES treatments for lignocellulose refinery in literature.

DES system	Raw lignocellulose	Lignocellulose refinery			Reference
		Cellulose	Hemicellulose	Lignin	
ChCl/OA/Diols	Poplar wood	Glucose, cellulose nanofibers	Xylose, furfural	Lignin polyols, monomers, printing resins	This work
BTMAC/LA	Corncob	Glucose	-	Not valorized	Ref (*25*)
ChCl/Gly/H_2SO_4	Switchgrass	Glucose	Xylose	Not valorized	Ref (*26*)
ChCl/LA	Switchgrass	Glucose	Xylose	-	Ref (*27*)
ChCl/EG/p-TSA	Switchgrass	Glucose	Xylose	Not valorized	Ref (*28*)
ChCl/EG/H_2SO_4	Switchgrass	Glucose, butanediol	Xylose, furfural	Not valorized	Ref (*29*)
ChCl/OA	Poplar wood	Cellulose nanocrystal	Xylose	Not valorized	Ref (*30*)
ChCl/LA	Eucalyptus	Glucose	Xylose	Not valorized	Ref (*31*)
ChCl/Gly	Corncob	Glucose	-	-	Ref (*32*)
ChCl/Gly/$AlCl_3 6H_2O$	Poplar wood	-	-	Not valorized	Ref (*33*)
ChCl/LA	Groundnut haulm	Ethanol	-	-	Ref (*34*)
ChCl/Urea	Rice straw	Characterized	-	-	Ref (*35*)
ChCl/PCA	Switchgrass	Glucose	Xylose	Not valorized	Ref (*36*)
ChCl/VAN ChCl/HBA	*Arabidopsis thaliana* stems	Glucose	Xylose	Not valorized	Ref (*37*)
ChCl/FA	Loblolly pine	Glucose	-	-	Ref (*38*)
ChCl/OA/$AlCl_3 6H_2O$ ChCl/LA/$AlCl_3 6H_2O$	Sugarcane bagasse	Cellulose nanofibers	-	-	Ref (*39*)
ChCl/FA	Corn stover	Glucose, butanol	-	-	Ref (*40*)
ChCl/BA/PEG-200	Wheat straw	Glucose	-	Not valorized	Ref (*41*)
ChCl/LA; ChCl/Lev	Poplar, Douglas fir	-	-	Not valorized	Ref (*42*)
ChCl/Imidazol	Corncob	Glucose	Xylose	-	Ref (*43*)
ChCl/Gly/$FeCl_3$	Hybrid pennisetum	-	-	Antioxidative lignin	Ref (*44*)
ChCl/PB	Poplar wood	Glucose	Xylose	Not valorized	Ref (*45*)
ChCl/OA/p-TSA	Thermomechanical pulp	Cellulose nanocrystals	-	-	Ref (*46*)
TEBAC/LA	Wheat straw	Glucose	Xylose	Not valorized	Ref (*47*)
ChCl/Gly/$FeCl_3$	Pennisetum	Glucose	-	-	Ref (*48*)

Table S2 Price of DES components and corresponding DESs.

Components	**Price ($ /ton)[a]**
Choline chloride	400–700
Oxalic acid dihydrate	780–850
Ethylene glycol	780–900
1,3-Propanediol	312–624
1,4-Butanediol	344–937
1,5-Pentanediol	390–470
COEG[b]	618–796
COPG[b]	521–738
COBD[b]	521–813
COPD[b]	527–686

[a] Prices of DES components were estimated from Alibaba.com.

[b] Prices of DESs were calculated according to the molar ratios of the corresponding DES; typical molar ratio was: ChCl: OA: diols = 1: 1: 1.

Table S3 Composition of control and DES fractionated SRs.(*2*)

Condition	SR (%)	SR composition (%)		Cellulose retention (%)	Hemicellulose removal (%)	Delignification (%)
		cellulose	hemicellulose			
Control	100	49.3±1.21	22.1±1.42	-	-	-
CO	50.3±1.8	86.5±5.61	1.7±0.08	88.3	92.3	75.1±1.48
COEG	54.8±0.9	87.3±1.06	4.4±0.12	97.0	89.1	91.9±0.56
COPG	53.7±1.08	85.3±3.94	5.7±0.27	92.9	86.1	95.4±0.55
COBD	54.5±1.37	90.8±1.11	5.8±0.26	99.5	85.7	95.8±0.13
COPD	53.5±0.81	91.5±2.62	6.0±0.36	99.3	85.5	96.4±0.41

Note: Glucose and xylose were used to determine the yield of cellulose and hemicellulose, and acid insoluble lignin was used to calculate the delignification.

Table S4 Semi-quantitative analysis of CO-L and COEG-L by 2D HSQC NMR.(*1*)

Lignin	Content / 100 aromatic units			Condensation ratio (%)
	β-*O*-4′ (A)	α-alkoxylated β-*O*-4′ (A′)	β-β′ (B)	
CO-L	0	0	0	53
COEG-L	1.3	5.1	2.2	41

Table S5 Assignment of the $^{13}C–^{1}H$ cross-signals in HSQC NMR spectra.(*49, 50*)

$^{13}C–^{1}H$ cross-signals	**^{1}H range/^{13}C range**
β-*O*-4_{α}	(4.76–5.10)/(73–77.5)
β'-*O*-4_{α}	(4.46–4.77)/(79.9–82.8)
β-*O*-4_{β} and β'-*O*-4_{β}	(4.03–4.23)/(84.1–86.4)
β-*O*-4_{γ} and β'-*O*-4_{γ}	(3.21–3.97)/(58.6–61.7)
β'-*O*-4_{diols}-C_{α}	(3.22–3.5)/(69.2–72.3)
β-5_{α}	(5.42–5.63)/(88–92)
β-5_{β}	(3.36–3.56)/(53–54.5)
β-5_{γ}	(3.50–4.00)/(62–64.5)
β-β_{α}	(4.59–4.77)/(86.5–89.5)
β-β_{β}	(2.98–3.20)/(55.5–59)
β-β_{γ}	(3.75–3.96)/(72.5–76)
	(4.10–4.31)/(72.5–76)
$S_{2/6}$	(6.48–6.90)/(104–109)
$S'_{2/6}$	(7.17–7.50)/(105–109)
$S_{condensed}$	(6.35–6.65)/(106–109)
G_2	(6.78–7.14)/(111.5–116)
G_5	(6.48–7.06)/(115–120.5)
G_6	(6.65–6.96)/(120.5–124.5)
$PB_{2/6}$	(7.51–7.97)/(130.5–132.4)

Table S6 Composition analysis of COPA-SR and COPD-SR.

DES	SR (%)	SR composition (%)		Delignification (%)
		Cellulose	Hemicellulose	
COPA	58.1±1.66	81.2±1.30	3.5±0.49	72.6±0.59
COPD	53.5±0.81	91.5±2.62	6.0±0.36	96.4±0.41

Note: Glucose and xylose are used to determine the yield of cellulose and hemicellulose, acid insoluble lignin is used to calculate the delignification.

Table S7 Semi-quantitative analysis of COEG-L, COPG-L, COBD-L and COPD-L by 2D HSQC NMR.(*50*)

Lignin	Content / 100 aromatic units			Total β-*O*-4′ content	Condensation ratio %
	β-*O*-4′ (A)	α-alkoxylated β-*O*-4′ (A′)	β-β′ (B)		
COEG-L	1.3	5.1	2.2	6.4	41
COPG-L	4	10.1	2.8	14.1	32
COBD-L	6	13.8	3.4	19.8	24
COPD-L	8.8	19.4	5.1	28.2	13

Table S8 Quantitative analysis of fractionated lignin by ^{31}P NMR.(*6*)

Lignin	Aliphatic OH(mmol/g)	Total phenolic OH (mmol/g)	Phenolic OH (mmol/g)			Carboxylic acid OH (mmol/g)
			G5 substituted	Guaiacyl	Hydroxyphenyl	
CO-L	0.07	2.78	2.18	0.5	0.05	0.05
COEG-L	1.47	3.05	2.07	0.70	0.22	0.06
COPG-L	1.51	2.20	1.41	0.43	0.15	0.21
COBD-L	1.70	1.49	1.03	0.37	0.09	0.17
COPD-L	1.85	1.35	0.81	0.31	0.08	0.15

Table S9 DP values of wood and fractionated SRs after 96 h.

SRs	Wood	CO-SR	COEG-SR	COPG-SR	COBD-SR	COPD-SR
DP	1280±8.8	475±0.9	526±4.4	723±2.5	753±3.5	859±0.9

Note: The DP was measured with a 1835-4-0.80 Ubbelohde viscometer (Xinbiao Tengda Instruments, Beijing, China), using copper(II)ethylenediamine as solvent.

Table S10 Glucose yield from enzymatic hydrolysis of SRs.

Time (h)	Glucose yield (%)					
	Wood	**CO-SR**	**COEG-SR**	**COPG-SR**	**COBD-SR**	**COPD-SR**
3	7.0 ±0.87	9.6 ±1.35	25.2 ±4.52	25.3 ±1.87	23.8 ±2.29	26.4 ±3.66
6	9.0 ±0.81	16.1 ±2.22	33.6 ±5.04	33.8 ±2.63	33.2 ±3.21	36.9 ±1.29
12	11.1 ±0.53	27.2 ±2.84	50.9 ±1.85	49.8 ±2.43	49.9 ±3.93	55.5 ±2.99
24	13.8 ±0.78	39.6 ±0.19	70.1 ±5.11	72.0 ±3.12	74.2 ±1.35	76.6 ±3.61
48	17.5 ±1.26	56.1 ±2.49	83.4 ±3.47	89.8 ±1.73	89.0 ±1.46	89.7 ±3.19
72	19.9 ±2.01	63.6 ±4.24	94.1 ±3.08	98.9 ±0.91	98.1 ±2.99	97.9 ±1.59
96	19.7 ±1.95	66.6 ±4.84	95.1 ±4.32	98.8 ±1.10	98.7 ±3.63	99.7 ±1.32

Table S11 Xylose yield from enzymatic hydrolysis of SRs after 96 h.

Time (h)	Xylose yield (%)					
	Wood	**CO-SR**	**COEG-SR**	**COPG-SR**	**COBD-SR**	**COPD-SR**
3	3.1 ±0.40	24.1 ±0.03	32.8 ±2.17	34.3 ±2.21	47.3 ±0.53	36.7 ±3.42
6	3.9 ±0.19	33.0 ±2.89	44.6 ±3.54	41.3 ±3.22	53.9 ±0.66	45.7 ±2.38
12	5.8 ±0.25	46.4 ±1.62	53.9 ±1.26	54.4 ±3.21	65.7 ±0.87	62.1 ±3.26
24	7.5 ±0.47	60.6 ±3.58	67.5 ±1.04	70.9 ±2.12	76.3 ±4.73	76.1 ±1.21
48	10.4 ±0.06	79.2 ±4.16	85.8 ±4.18	83.7 ±1.06	90.7 ±3.84	92.2 ±4.65
72	11.0 ±0.60	89.6 ±1.28	96.7 ±2.85	91.7 ±1.22	96.7 ±1.14	98.7 ±1.76
96	11.1 ±0.69	95.7 ±3.27	99.2 ±1.46	95.9 ±1.49	97.8 ±0.39	98.9 ±2.49

Table S12 Comparative investigation of the enzymatic hydrolyzed glucose yield in literature.

Biomass	DES systems	Delignification (%)	Glucose yield to initial glucan in biomass (%)	References
Poplar	COEG	91.9±0.56	95.1±4.3	This work
Poplar	COPG	95.4±0.55	98.8±1.1	This work
Poplar	COBD	95.8±0.13	98.7±3.6	This work
Poplar	COPD	96.4±0.41	99.7±1.3	This work
Rice straw	Lac-Guanidine HCl	31	79	Ref (*51*)
Corncobs	Bet-AA	50	60.8	Ref (*52*)
Corncobs	ChCl-imidazole	50.6	85	Ref (*43*)
Bagasse	ChCl-Lac	50.6	86	Ref (*53*)
Poplar	ChCl-*p*-HBA	69	71	Ref (*45*)
Corncobs	BTMAC-Lac	63.4	91	Ref (*25*)
Miscanthus	ChCl-Lac	65.2	28.8	Ref (*27*)
Corncobs	ChCl-Lac	79.6	59.3	Ref (*27*)
Rice straw	CO-CU	68	81	Ref (*54*)
Eucalyptus	ChCl-Lac	80.2	78.4	Ref (*31*)
Pennisetum	ChCl-Gly-$FeCl_3$	78.9	80.5	Ref (*48*)
Wheat straw	ChCl-PEG-BA	88.4	59.3	Ref (*55*)
Bamboo	ChCl-EG-*p*-TsOH	90.3	78.1	Ref (*56*)

Table S13 Value of lignocellulose and refinery products.

Raw lignocellulose or product	Price ($/ton)[a]
Poplar sawdust	50–100
Pulp	800
Cellulose nanofibers	9000–11,000[b]
Cellulose nanocrystals	38,000–40,000[b]
Glucose	520
Xylose	1000
Furfural	1200
Phenol	1750[c]
Vanillin	6000
Aromatic polyols	1700–2000[d]
Lignin-derived oligomers	2000[c]

[a] Price of products from Alibaba.com.

[b] Prices of cellulose nanofiber and cellulose nanocrystal from Beijing Dingsheng Brothers Technology Co., Ltd.; solid content of the nanocellulose was 2 wt%.

[c] Values from the literature.(*57*)

[d] Obtained lignin can be directly used as a substitute for aromatic polyols.

Table S14 Yields of SRs and lignin from fractionation using recycled DES.

DES fractionation[a]	First round	Second round	Third round	Fourth round
SR yield (%)	54.1	55.4	57.4	59.3
Lignin yield (%)	69.8	67.3	67.1	64.5

[a] Data given as mean values; $n = 3$.

Table S15 Composition analysis of SRs from fractionation using recycled DES.

DES	Cellulose retention (%)	Hemicellulose retention (%)	Delignification (%)
COPD	96.0 ± 0.25	15.7 ± 0.45	93.2 ± 0.70
COPD-R1	92.6 ± 0.92	14.8 ± 0.50	92.7 ± 0.67
COPD-R2	93.2 ± 0.68	7.2 ± 0.57	90.4 ± 0.54
COPD-R3	92.3 ± 1.63	7.1 ± 1.37	84.7 ± 1.13

Table S16 Composition analysis of SR from increased amount of lignocellulose (by 5 times) for fractionation in COPD.

COPD	SR (%)	Cellulose retention (%)	Hemicellulose retention (%)	Delignification (%)
Scale fractionation	56%	95.8 ±0.50	19.9 ±0.99	89.6 ±1.10

References

1. D. S. Zijlstra, C. W. Lahive, C. A. Analbers, M. B. Figueirêdo, Z. Wang, C. S. Lancefield, P. J. Deuss, Mild Organosolv Lignin Extraction with Alcohols: The Importance of Benzylic Alkoxylation. *ACS Sustain. Chem. Eng.* **8**, 5119–5131 (2020).
2. A. Sluiter, B. Hames, R. Ruiz, C. Scarlata, J. Sluiter, D. Templeton, D. Crocker, Determination of structural carbohydrates and lignin in Biomass. *Lab. Anal. Proced.*, 17 (2012).
3. G. Toscano, G. Riva, E. Foppa Pedretti, F. Corinaldesi, C. Mengarelli, D. Duca, Investigation on wood pellet quality and relationship between ash content and the most important chemical elements. *Biomass and Bioenergy*. **56**, 317–322 (2013).
4. A. Björkman, Studies on finely divided wood. Part 1. Extraction of lignin with neutral solvents. *Sven. Papperstidn*. **59**, 477–485 (1956).
5. J. Rencoret, G. Marques, A. Gutiérrez, L. Nieto, J. Rio, Isolation and structural characterization of the milled-wood lignin from Paulownia fortunei wood. *Ind. Crops Prod.* **30**, 137–143 (2009).
6. J.-L. Wen, S.-L. Sun, B.-L. Xue, R.-C. Sun, Quantitative structures and thermal properties of birch lignins after ionic liquid pretreatment. *J. Agric. Food Chem.* **61**, 635–645 (2013).
7. T. Ren, S. You, Z. Zhang, Y. Wang, W. Qi, R. Su, Z. He, Highly selective reductive catalytic fractionation at atmospheric pressure without hydrogen. *Green Chem.* **23**, 1648–1657 (2021).
8. S. H. Jung, S. J. Kim, J. S. Kim, Characteristics of products from fast pyrolysis of fractions of waste square timber and ordinary plywood using a fluidized bed reactor. *Bioresour. Technol.* **114**, 670–676 (2012).
9. Y.-B. Ha, M. Jin, S.-S. Oh, D. Ryu, Synthesis of an Environmentally Friendly Phenol-Free Resin for Printing Ink. *Bull. Korean Chem. Soc.* **33**, 3413–3416 (2012).
10. G. Akay, C. A. Jordan, Gasification of fuel cane bagasse in a downdraft gasifier: Influence of lignocellulosic composition and fuel particle size on syngas composition and yield. *Energy and Fuels*. **25**, 2274–2283 (2011).
11. B. H. R. Suryanto, H. L. Du, D. Wang, J. Chen, A. N. Simonov, D. R. MacFarlane, Challenges and prospects in the catalysis of electroreduction of nitrogen to ammonia. *Nat. Catal.* **2**, 290–296 (2019).
12. J. Baeyens, Q. Kang, L. Appels, R. Dewil, Y. Lv, T. Tan, Challenges and opportunities in improving the production of bio-ethanol. *Prog. Energy Combust. Sci.* **47**, 60–88 (2015).
13. J. L. Guil, M. E. Torija, J. J. Giménez, I. Rodríguez-García, A. Giménez, Oxalic acid and calcium determination in wild edible plants. *J. Agric. Food Chem.* **44**, 1821–1823 (1996).
14. R. S. Costa, B. S. R. Aranha, A. Ghosh, A. O. Lobo, E. T. S. G. da Silva, D. C. B. Alves, B. C. Viana, Production of oxalic acid by electrochemical reduction of CO_2 using silver-carbon material from babassu coconut mesocarp. *J. Phys. Chem. Solids*. **147**, 109678 (2020).
15. M. Kumar, Oxalic acid production by Aspergillus niger. *Int. J. Pharma Bio Sci.* **4**, 337-342 (2013).
16. S. K. Mandal, P. C. Banerjee, Submerged production of oxalic acid from glucose by immobilized Aspergillus niger. *Process Biochem.* **40**, 1605–1610 (2005).
17. A. Wang, T. A. O. Zhang, One-Pot Conversion of Cellulose Tungsten-Based Catalysts. **46**, 1377–1386 (2013).

18. Y. Liu, C. Luo, H. Liu, Tungsten Trioxide Promoted Selective Conversion of Cellulose into Propylene Glycol and Ethylene Glycol on a Ruthenium Catalyst. *Angew. Chemie*. **124**, 3303–3307 (2012).
19. Y. Nakagawa, Y. Shinmi, S. Koso, K. Tomishige, Direct hydrogenolysis of glycerol into 1,3-propanediol over rhenium-modified iridium catalyst. *J. Catal.* **272**, 191–194 (2010).
20. F. S. Mendes, M. Gonz âlez-Pajuelo, H. Cordier, J. M. Fran çois, I. Vasconcelos, 1,3-Propanediol production in a two-step process fermentation from renewable feedstock. *Appl. Microbiol. Biotechnol.* **92**, 519–527 (2011).
21. A. Burgard, M. J. Burk, R. Osterhout, S. Van Dien, H. Yim, Development of a commercial scale process for production of 1,4-butanediol from sugar. *Curr. Opin. Biotechnol.* **42**, 118–125 (2016).
22. W. Xu, H. Wang, X. Liu, J. Ren, Y. Wang, G. Lu, Direct catalytic conversion of furfural to 1,5-pentanediol by hydrogenolysis of the furan ring under mild conditions over Pt/Co2AlO4 catalyst. *Chem. Commun.* **47**, 3924–3926 (2011).
23. K. Huang, Z. J. Brentzel, K. J. Barnett, J. A. Dumesic, G. W. Huber, C. T. Maravelias, Conversion of Furfural to 1,5-Pentanediol: Process Synthesis and Analysis. *ACS Sustain. Chem. Eng.* **5**, 4699–4706 (2017).
24. L. Segal, J. J. Creely, A. E. Martin, C. M. Conrad, An Empirical Method for Estimating the Degree of Crystallinity of Native Cellulose Using the X-Ray Diffractometer. *Text. Res. J.* **29**, 786–794 (1959).
25. Z. Guo, Q. Zhang, T. You, X. Zhang, F. Xu, Y. Wu, Short-time deep eutectic solvent pretreatment for enhanced enzymatic saccharification and lignin valorization. *Green Chem.* **21**, 3099–3108 (2019).
26. Z. Chen, W. D. Reznicek, C. Wan, Deep eutectic solvent pretreatment enabling full utilization of switchgrass. *Bioresour. Technol.* **263**, 40–48 (2018).
27. Z. Chen, C. Wan, Ultrafast fractionation of lignocellulosic biomass by microwave-assisted deep eutectic solvent pretreatment. *Bioresour. Technol.* **250**, 532–537 (2018).
28. Z. Chen, W. A. Jacoby, C. Wan, Ternary deep eutectic solvents for effective biomass deconstruction at high solids and low enzyme loadings. *Bioresour. Technol.* **279**, 281–286 (2019).
29. Z. Chen, X. Bai, A. Lusi, C. Wan, High-Solid Lignocellulose Processing Enabled by Natural Deep Eutectic Solvent for Lignin Extraction and Industrially Relevant Production of Renewable Chemicals. *ACS Sustain. Chem. Eng.* **6**, 12205-12216 (2018).
30. Y. Liu, W. Chen, Q. Xia, B. Guo, Q. Wang, S. Liu, Y. Liu, J. Li, H. Yu, Efficient Cleavage of Lignin–Carbohydrate Complexes and Ultrafast Extraction of Lignin Oligomers from Wood Biomass by Microwave-Assisted Treatment with Deep Eutectic Solvent. *ChemSusChem*. **10**, 1692–1700 (2017).
31. X. J. Shen, J. L. Wen, Q. Q. Mei, X. Chen, D. Sun, T. Q. Yuan, R. C. Sun, Facile fractionation of lignocelluloses by biomass-derived deep eutectic solvent (DES) pretreatment for cellulose enzymatic hydrolysis and lignin valorization. *Green Chem.* **21**, 275-283 (2019).
32. C.-W. Zhang, S.-Q. Xia, P.-S. Ma, Facile pretreatment of lignocellulosic biomass using deep eutectic solvents. *Bioresour. Technol.* **219**, 1–5 (2016).
33. Q. Xia, Y. Liu, J. Meng, W. Cheng, W. Chen, S. Liu, Y. Liu, J. Li, H. Yu, Multiple hydrogen bond coordination in three-constituent deep eutectic solvents enhances lignin fractionation from biomass. *Green Chem.* **20**, 2711–2721 (2018).

34. S. I. Okuofu, A. S. Gerrano, S. Singh, S. Pillai, Deep eutectic solvent pretreatment of Bambara groundnut haulm for enhanced saccharification and bioethanol production. *Biomass Convers. Biorefinery* (2020), doi:10.1007/s13399-020-01053-w.
35. M. Pan, G. Zhao, C. Ding, B. Wu, Z. Lian, H. Lian, Physicochemical transformation of rice straw after pretreatment with a deep eutectic solvent of choline chloride/urea. *Carbohydr. Polym.* **176**, 307–314 (2017).
36. K. H. Kim, T. Dutta, J. Sun, B. Simmons, S. Singh, Biomass pretreatment using deep eutectic solvents from lignin derived phenols. *Green Chem.* **20**, 809–815 (2018).
37. K. H. Kim, A. Eudes, K. Jeong, C. G. Yoo, C. S. Kim, A. Ragauskas, Integration of renewable deep eutectic solvents with engineered biomass to achieve a closed-loop biorefinery. *Proc. Natl. Acad. Sci.* **116**, 13816–13824 (2019).
38. J. G. Lynam, N. Kumar, M. J. Wong, Deep eutectic solvents' ability to solubilize lignin, cellulose, and hemicellulose; thermal stability; and density. *Bioresour. Technol.* **238**, 684–689 (2017).
39. Q. Ji, X. Yu, A. E. G. A. Yagoub, L. Chen, C. Zhou, Efficient cleavage of strong hydrogen bonds in sugarcane bagasse by ternary acidic deep eutectic solvent and ultrasonication to facile fabrication of cellulose nanofibers. *Cellulose*. **28**, 6159–6182 (2021).
40. G. C. Xu, J. C. Ding, R. Z. Han, J. J. Dong, Y. Ni, Enhancing cellulose accessibility of corn stover by deep eutectic solvent pretreatment for butanol fermentation. *Bioresour. Technol.* **203**, 364–369 (2016).
41. Y. Ci, F. Yu, C. Zhou, H. Mo, Z. Li, Y. Ma, L. Zang, New ternary deep eutectic solvents for effective wheat straw deconstruction into its high-value utilization under near-neutral conditions. *Green Chem.* **22**, 8713-8720 (2020).
42. C. Alvarez-Vasco, R. Ma, M. Quintero, M. Guo, S. Geleynse, K. K. Ramasamy, M. Wolcott, X. Zhang, Unique low-molecular-weight lignin with high purity extracted from wood by deep eutectic solvents (DES): a source of lignin for valorization. *Green Chem.* **18**, 5133–5141 (2016).
43. A. Procentese, E. Johnson, V. Orr, A. Garruto Campanile, J. A. Wood, A. Marzocchella, L. Rehmann, Deep eutectic solvent pretreatment and subsequent saccharification of corncob. *Bioresour. Technol.* **192**, 31–36 (2015).
44. Z. K. Wang, S. Hong, J. long Wen, C. Y. Ma, L. Tang, H. Jiang, J. J. Chen, S. Li, X. J. Shen, T. Q. Yuan, Lewis Acid-Facilitated Deep Eutectic Solvent (DES) Pretreatment for Producing High-Purity and Antioxidative Lignin. *ACS Sustain. Chem. Eng.* **8**, 1050–1057 (2020).
45. Y. Wang, X. Meng, K. Jeong, S. Li, G. Leem, K. H. Kim, Y. Pu, A. J. Ragauskas, C. G. Yoo, Investigation of a lignin-based deep eutectic solvent using p-hydroxybenzoic acid for efficient woody biomass conversion. *ACS Sustain. Chem. Eng.* **8**, 12542–12553 (2020).
46. J. Jiang, N. C. Carrillo-Enr ́quez, H. Oguzlu, X. Han, F. Jiang, High Production Yield and More Thermally Stable Lignin-Containing Cellulose Nanocrystals Isolated Using a Ternary Acidic Deep Eutectic Solvent. *ACS Sustain. Chem. Eng.* **8**, 7182–7191 (2020).
47. Y. Liu, J. Zheng, J. Xiao, X. He, K. Zhang, S. Yuan, Z. Peng, Z. Chen, X. Lin, Enhanced Enzymatic Hydrolysis and Lignin Extraction of Wheat Straw by Triethylbenzyl Ammonium Chloride/Lactic Acid-Based Deep Eutectic Solvent Pretreatment. *ACS Omega* 4, 19829–19839 (2019).

48. Z. K. Wand, H. Li, X. C. Lin, L. Tang, J. J. Chen, J. W. Mo. R. S. Yu. X. J. Shen, Novel recyclable deep eutectic solvent boost biomass pretreatment for enzymatic hydrolysis. *Bioresour. Technol.* **307**, 123237 (2020).
49. C. S. Lancefield, I. Panovic, P. J. Deuss, K. Barta, N. J. Westwood, Pre-treatment of lignocellulosic feedstocks using biorenewable alcohols: Towards complete biomass valorisation. *Green Chem.* **19**, 202–214 (2017).
50. D. Wang, W. Wang, W. Lv, Y. Xu, J. Liu, H. Wang, C. Wang, L. Ma, The Protection of C−O Bond of Pine Lignin in Different Organic Solvent Systems. *ChemistrySelect*. **5**, 3850–3858 (2020).
51. X. D. Hou, A. L. Li, K. P. Lin, Y. Y. Wang, Z. Y. Kuang, S. L. Cao, Insight into the structure-function relationships of deep eutectic solvents during rice straw pretreatment. *Bioresour. Technol.* **249**, 261–267 (2018).
52. Y. Liang, W. Duan, X. An, Y. Qiao, Y. Tian, H. Zhou, Novel betaine-amino acid based natural deep eutectic solvents for enhancing the enzymatic hydrolysis of corncob. *Bioresour. Technol.* **310**, 123389 (2020).
53. V. R. Chourasia, A. Pandey, K. K. Pant, R. J. Henry, Improving enzymatic digestibility of sugarcane bagasse from different varieties of sugarcane using deep eutectic solvent pretreatment. *Bioresour. Technol.* **337**, 125480 (2021).
54. X. D. Hou, G. J. Feng, M. Ye, C. M. Huang, Y. Zhang, Significantly enhanced enzymatic hydrolysis of rice straw via a high-performance two-stage deep eutectic solvents synergistic pretreatment. *Bioresour. Technol.* **238**, 139–146 (2017).
55. Y. H. Ci, F. Yu, C. X. Zhou, H. E. Mo, Z. Y. Li, Y. Q. Ma, L. H. Zang, New ternary deep eutectic solvents for effective wheat straw deconstruction into its high-value utilization under near-neutral conditions. *Green Chem.* **22**, 8713–8720 (2020).
56. Q. Zhai, F. Long, X. Jiang, C. yun Hse, J. Jiang, J. Xu, Facile and rapid fractionation of bamboo wood with a p-toluenesulfonic acid-based three-constituent deep eutectic solvent. *Ind. Crops Prod.* **158**, 113018 (2020).
57. Y. Liao, S.-F. Koelewijn, G. den Bossche, J. Van Aelst, S. den Bosch, T. Renders, K. Navare, T. Nicola, K. Van Aelst, M. Maesen, H. Matsushima, J. M. Thevelein, K. Van Acker, B. Lagrain, D. Verboekend, B. F. Sels, A sustainable wood biorefinery for low carbon footprint chemicals production. *Science* **367**, 1385–1390 (2020).